Chapter 2

THEORETICAL BACKGROUND

2.1. Concepts and Definitions

2.1.1. Radiometric Concepts

Two basic radiometric parameters are commonly used to describe the distribution of light field: radiance and irradiance. The definitions of the radiometric parameters used in this thesis are as follows [*Kirk*, 1984; Mobley, 1994]:

Radiance L(θ,ϕ,λ): The radiant power in a beam per unit solid angle per unit area perpendicular to the beam per unit wavelength interval.

Irradiance E(λ): The radiant power per unit area per unit wavelength interval.

Upward irradiance $E_u(\lambda)$: The upward directed radiant power per unit area onto an downward facing horizontal surface.

Downward irradiance $E_d(\lambda)$: The downward directed radiant power per unit area onto an upward facing horizontal surface.

$E_u(\lambda)$ and $E_d(\lambda)$can be derived by the integration of $L(\theta,\phi,\lambda)$ over appropriate angles:

$$E_u(\lambda) = \int_{\phi=0}^{2\pi}\int_{\theta=0}^{\pi/2} L(\theta,\phi,\lambda)\cos\theta\sin\theta\, d\theta\, \mathrm{d}\phi\,, \tag{2.1}$$

$$E_d(\lambda) = \int_{\phi=0}^{2\pi}\int_{\theta=\pi/2}^{\pi} L(\theta,\phi,\lambda)\cos\theta\sin\theta\, d\theta\, \mathrm{d}\phi\,, \tag{2.2}$$

where θ is the zenith angle, and ϕ is the azimuth angle.

2.1.2. Inherent Optical Properties

There are two types of optical properties of water: the inherent optical properties (IOPs) and the apparent optical properties (AOPs). IOPs solely depend on the type and the concentration of substance present in water, are independent of the ambient light field within the water. AOPs depend both on the type and the concentration of substance present in water and on the geometric structure of the ambient light field. AOPs can be derived from the measurements taken by an ocean colour sensor. The radiative transfer theory provides the connection between the AOPs and the IOPs. In this subsection, IOPs are introduced, and AOPs will be described in the next subsection.

The fundamental IOPs are the absorption coefficient and the volume scattering function. Other IOPs, such as the scattering coefficient, the beam attenuation coefficient and the single-scattering albedo, can be derived from these two fundamental IOPs.

The spectral absorption coefficient a(λ) is defined as the spectral absorptance per unit distance of photon travel in a dielectric medium.

The spectral scattering coefficient b(λ) is defined as the spectral scatterance per unit distance of photon travel in a dielectric medium.

The spectral beam attenuation coefficient c(λ) is defined as the sum of a(λ) and b(λ).

The spectral volume scattering function β(θ, λ) is defined as the ratio of the scattered spectral radiance to the incident spectral irradiance per unit volume.

Integrating β(θ,λ) over all directions gives the spectral scattering coefficient. It can be expressed as:

$$b(\lambda) = 2\pi \int_0^{\pi} \beta(\theta, \lambda) \sin(\theta) d\theta \tag{2.3}$$

The spectral scattering coefficient can be divided into two parts: the forward spectral scattering coefficient, b_f, relating to light scattered from the beam in a forward direction, and the spectral back scattering coefficient, b_b, relating to light scattered from the beam in a backward direction. They are expressed as,

$$b_b(\lambda) = 2\pi \int_{\pi/2}^{\pi} \beta(\theta, \lambda) \sin(\theta) d\theta \tag{2.4}$$

$$b_f(\lambda) = 2\pi \int_0^{\pi/2} \beta(\theta, \lambda) \sin(\theta) d\theta \tag{2.5}$$

The spectral phase function, $\tilde{\beta}(\theta, \lambda)$ is defined as the ratio of the spectral volume scattering function to the spectral scattering coefficient. Hence, integral of $\tilde{\beta}(\theta, \lambda)$ over all solid angles is equal to 1.

Forward scattering probability $\tilde{b}_f(\lambda)$ and back scattering probability $\tilde{b}_b(\lambda)$ are defined as,

$$\tilde{b}_f(\lambda) \equiv \frac{b_f(\lambda)}{b(\lambda)}, \tag{2.6}$$

$$\tilde{b}_b(\lambda) \equiv \frac{b_b(\lambda)}{b(\lambda)}. \tag{2.7}$$

Another inherent optical property commonly used is the spectral single scattering albedo, $\omega_0(\lambda)$, defined as the ratio of the spectral scattering coefficient to the spectral bean attenuation coefficient c(λ):

$$\omega_0(\lambda) \equiv \frac{b(\lambda)}{c(\lambda)}, \tag{2.8}$$

where c(λ)=a(λ)+b(λ).

The single scattering albedo is also known as the probability of photon survival.

2.1.3. Apparent Optical Properties

Two apparent optical properties are commonly used to represent the intrinsic colour of the ocean: hemispherical reflectance R(λ) and remote sensing reflectance $R_{RS}(\lambda)$.

The spectral hemispherical reflectance is defined as the ratio of spectral upward to downward irradiance:

$$R(\lambda, z) \equiv \frac{E_u(\lambda, z)}{E_d(\lambda, z)} \tag{2.9}$$

R(λ, z) is often evaluated in the water just below the surface ($z=0^-$).

The spectral remote sensing reflectance R_{RS} is defined as the ratio of the water leaving radiance to the downward irradiance just above the sea surface($z=0^+$):

$$R_{RS}(\theta, \phi, \lambda) \equiv \frac{L_w(\theta, \phi, \lambda)}{E_d(\lambda)} \tag{2.10}$$

The spectral remote sensing reflectance specifies that portion of downward light incident onto the water surface which is returned through the surface into direction (θ,ϕ).

The Q factor is defined as the ratio of upwelling irradiance to upwelling radiance just below the sea surface:

$$Q = \frac{E_u}{L_u} \tag{2.11}$$

If the L_u distribution were isotropic that is independent on the direction of propagation, Q would equal π. Actually, Q is a function of solar zenith angle, observation angle, as well as the wavelength [*Morel and Gentili*, 1993, 1996].

2.2. Optical Properties of Sea Water

In order to study the absorbing and scattering properties of natural waters, it is necessary to know the composition of those waters.

Constituents of natural waters are traditionally divided into particulate matter and dissolved matter. When filtering a water sample, everything that passes through a filter whose pore size is on the order of 0.4 μm is called dissolved matter, and everything retained on the filter is called particulate matter. The composition of particulate matter is very complex. It is divided into organic and inorganic particles, or living and non-living particles, or endogenous and exogenous particles for different purposes. In this study, suspended particulate matter is divided into endogenous and exogenous particles. The endogenous particles consist of phytoplankton and other associated particles, such as detritus, bacteria produced locally in a water body. The exogenous particles consist of sediments brought by rivers, re-suspended from the shallow bottom, and dust-settled from the atmosphere.

The dissolved organic matter is mostly produced during the decay of plant matter. The coloured fraction of it consists mostly of various humic and fulvic acids and is referred to as coloured dissolved organic matter (CDOM), or yellow matter, gilvin, and gelbstoff, because of the properties of spectral absorption. Based on the different sources, it is divided into endogenous and exogenous CDOM. The endogenous CDOM is associated with biological activity in ocean, while the exogenous CDOM comes from land drainage, and is mainly produced by the decay of terrestrial vegetation. The concentrations of exogenous CDOM are mostly higher in the coastal waters influenced by river discharge.

The absorption coefficient of water a(λ) can be separated into individual contributions by different water constituents:

$$a(\lambda) = a_w(\lambda) + a_{p1}(\lambda) + a_{p2}(\lambda) + a_{y1}(\lambda) + a_{y2}(\lambda), \tag{2.12}$$

where the subscripts w, p1, p2, y1 and y2, respectively, indicate pure sea water, endogenous particles, exogenous particles, endogenous CDOM, and exogenous CDOM.

The total scattering coefficient of natural water is modelled as the sum of the scattering coefficients of pure seawater and particles:

$$b(\lambda) = b_w(\lambda) + b_p(\lambda) \tag{2.13}$$

The phase function of natural water depends on the phase function of the various scattering substances and their relative contribution to the total scattering coefficient:

$$\tilde{\beta}(\lambda) = (b_w(\lambda) \times \tilde{\beta}_w(\lambda) + b_p(\lambda) \times \tilde{\beta}_p(\lambda)) / (b_w(\lambda) + b_p(\lambda)) \tag{2.14}$$

2.2.1. Pure Seawater

The absorption coefficient of pure seawater $a_w(\lambda)$ has been measured with sufficient accuracy for most applications. The *Pope and Fry* (1997) absorption values in the wavelength range 380 nm to 709 nm are widely used. For wavelengths above 709nm, the *Hale and Querry* (1973) absorption values are commonly taken. They are shown in Figure 2.1.

The scattering coefficient of pure seawater $b_w(\lambda)$ (Figure 2.2) is taken from *Morel* (1974):

$$b_w(\lambda) = 0.00288\left(\frac{\lambda}{500}\right)^{-4.32} \tag{2.15}$$

The phase function $\tilde{\beta}_w(\theta, \lambda)$ (Figure 2.3) was given by (*Morel*, 1974):

$$\tilde{\beta}_w(\theta) = 0.06225(1 + 0.835\cos^2\theta) \tag{2.16}$$

2.2.2. Phytoplankton

Phytoplankton cells are strong absorbers of visible light and therefore play a major role in determining the absorption of natural waters. The spectral absorption properties of phytoplankton have been widely studied [*Prieur and Sathyendranath*, 1981; *Morel*, 1988; *Carder et al*., 1991; *Hoepffner and Sathyendranath,* 1993; *Bricaud et. al*., 1995; *Bricaud et al*., 1998; *Kondratyev et*

al., 1998]. These studies show that the phytoplankton absorption has several general features: there are distinct absorption peaks around 440 nm and 675 nm; there is relatively little absorption between 550 and 650 nm.

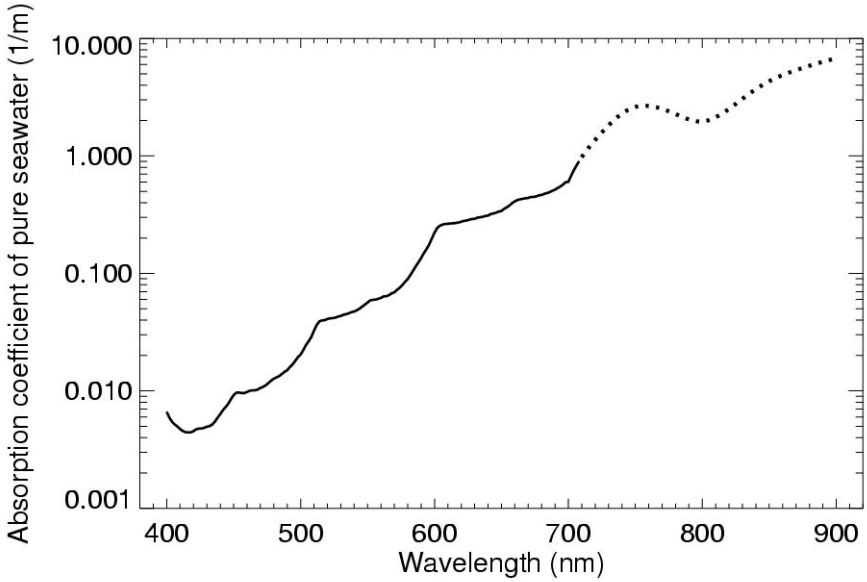

Figure 2.1. The absorption coefficient of pure seawater (λ=380-709 nm from *Pope and Fry* (1994), λ > 709 nm from *Hale and Querry* (1973)).

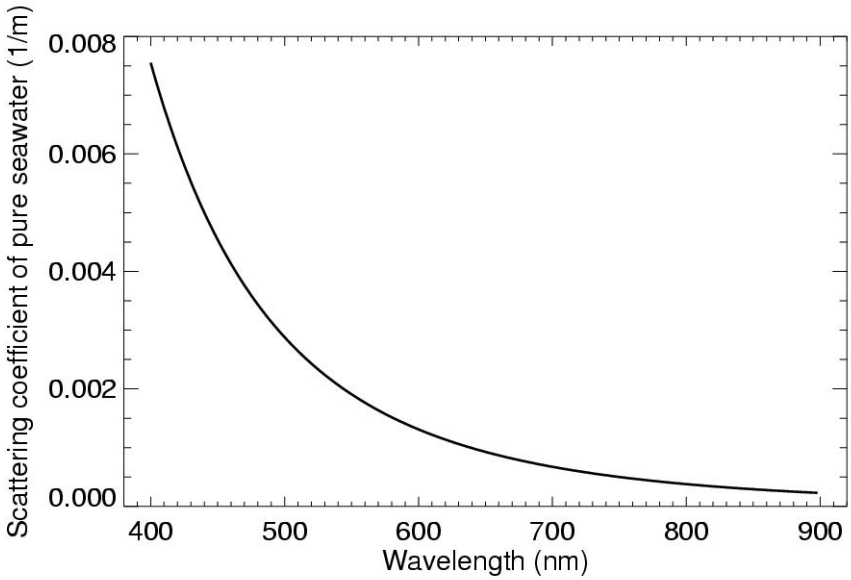

Figure 2.2. The scattering coefficient of pure seawater, from *Morel* (1974)

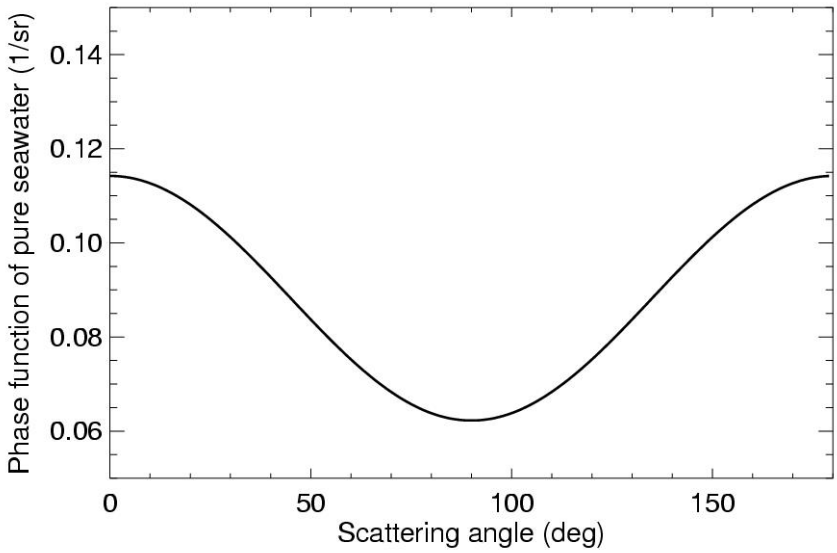

Figure 2.3. The phase function of pure seawater, from *Morel* (1974)

Bricaud et al. (1995) developed an empirical relationship between the chlorophyll-a specific absorption coefficient of phytoplankton $a^*_{ph}(\lambda)$ and the chlorophyll concentration from a data set including 815 spectra determined with the wet filter technique in different regions of the world ocean (covering the range of chlorophyll concentration 0.02-25 μg/l). It is expressed as:

$$a^*_{ph}(\lambda) = A(\lambda) < chla >^{-B(\lambda)}, \tag{2.17}$$

where A(λ) and B(λ) are positive, wavelength-dependent parameters.

Based on 1116 spectra of endogenous particles, *Bricaud et al*. (1998) derived a power function to represent the relationship between the absorption coefficient of endogenous particles (i.e. phytoplankton plus detritus particles) and the chlorophyll concentration:

$$a_p(\lambda) = A_p(\lambda) < CHL >^{-E_p(\lambda)}, \tag{2.18}$$

where $A_p(\lambda)$and $E_p(\lambda)$ are positive, wavelength-dependent parameters.

Figure 2.2 shows the spectral absorption coefficient of endogenous particles for CHL =1 mg m^{-3}, based on Eq. (2.18).

Several models are available for the total scattering coefficient $b_p(\lambda)$ of endogenous particles (*Gordon and Morel*, 1983 ; *Loisel and Morel*, 1998).

Based on a large dataset (N = 2,787) made up of recent measurements of the beam attenuation coefficient at 660 nm and of the chlorophyll concentration in Case I waters, *Loisel and Morel* (1998) proposed a power law relating the pigment concentration to the beam attenuation coefficient:

$$c_p(660) = \alpha \left[CHL\right]^{\beta} \tag{2.19}$$

At 660 nm, about 97 % of the particle beam attenuation coefficient is caused by scattering [*Loisel and Morel*, ibid]. At this wavelength, the scattering coefficient may therefore be assumed identical to the beam attenuation coefficient. Recent *in-situ* measurements show that the wavelength dependence of scattering by marine particles is low or is even not observed [*Barnard et al.,* 1998*; Gould et al.,* 1999*; Babin et al.,* 2000]. Therefore, the scattering of marine particles is assumed to be independent of wavelength within the considered domain, expressed as:

$$b_p = A_{bp}\left[CHL\right]^{B_{bp}}, \tag{2.20}$$

where the coefficients A_{bp}=0.252 and B_{bp}=0.635 were derived from 610 measurements in the homogeneous surface layer taken in the tropical and subtropical Atlantic and Pacific Oceans and the Mediterranean Sea [*Loisel and Morel*, ibid.]. In this study, Eq. (2.20) is taken as the model for the scattering coefficient of endogenous particles.

The model of Gordon and Morel [1983] is given by:

$$b_p(\lambda) = 0.3 < chl >^{0.62} \left(\frac{550}{\lambda}\right) \tag{2.21}$$

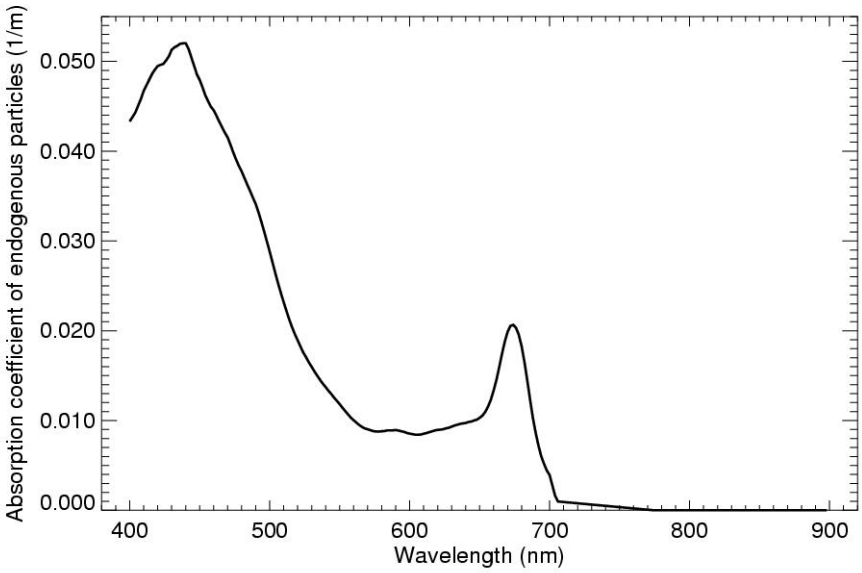

Figure 2.4. The absorption coefficient of endogenous particles for CHL=1 mg m^{-3}, based on Eq. 2.18.

2.2.3. Suspended particulate matter

Based on the absorption properties of nonalgal particles (NAP) measured at about 350 stations in various coastal waters around Europe including the English Channel, Adriatic Sea, Baltic Sea, Mediterranean Sea, and North Sea, absorption spectra of these particles were well described by an exponential function [*Babin,* 2000]:

$$a_{nap}(\lambda) = a_{nap}(443)\exp^{-s(\lambda-443)}, \tag{2.22}$$

$$a_{nap}(443) = 0.0216 < SPM >^{1.0247}, \tag{2.23}$$

where s is empirically determined, an average value of 0.0123 nm^{-1} with SD = 0.0013 nm^{-1}. SPM is the concentration of total suspended matter, in g m^{-3}. Figure 2.5 shows the spectral absorption coefficient of exogenous particles for SPM = 3 g m^{-3}, based on Eq. (2.22) and (2.23).

The scattering coefficient of total suspended particulate matter in Case II waters (endogenous plus exogenous particles) $b_p(\lambda)$ can be expressed as [*Babin*, 2000]:

$$b_p(\lambda) = b_p(550) \tag{2.24}$$

$$b_p(550) = 0.5 < SPM > \tag{2.25}$$

The above relationships were derived based the measurements taken at 250 different coastal sites located in the English Channel, Adriatic Sea, Baltic Sea, Mediterranean Sea, and North Sea.

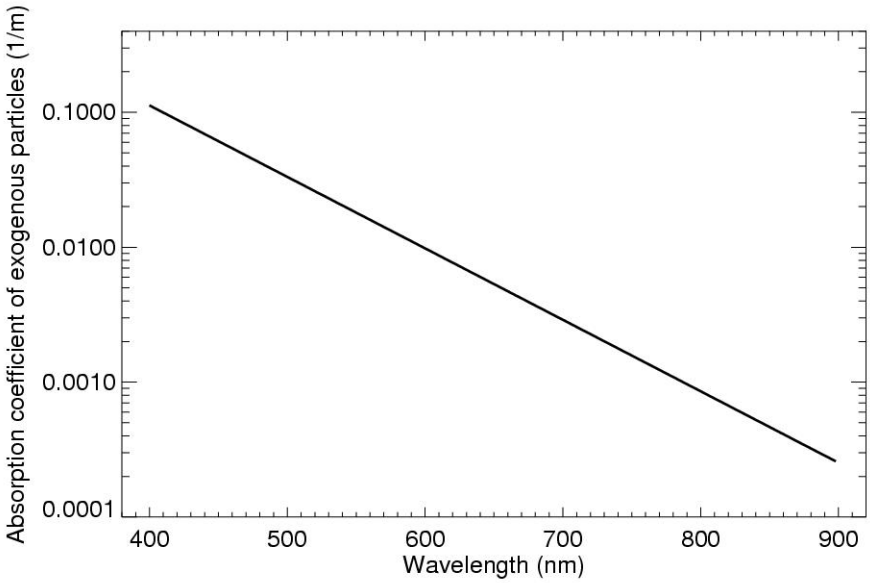

Figure 2.5. The absorption coefficient of exogenous particles for SPM= 3 g m^{-3}, based on Eq. (2.22) and (2.23).

Although commercial instruments for measuring the angular distribution of scattered light *in-situ* are meanwhile becoming available [*Pegau et al.*, 2001], measurements of the volume scattering function or the back scattering probability for marine particles are still scare. The phase function for marine particles still mostly used in ocean optics has been derived by *Mobley et al.* (1993) based on measurements taken in San Diego Harbour and San Diego Bay [*Petzold*, 1972]. Figure 2.6 shows the volume scattering functions for three oceanic waters [*Petzold*, 1972] and particles phase function derived by *Mobley et al.* (1993), all at λ=514 nm.

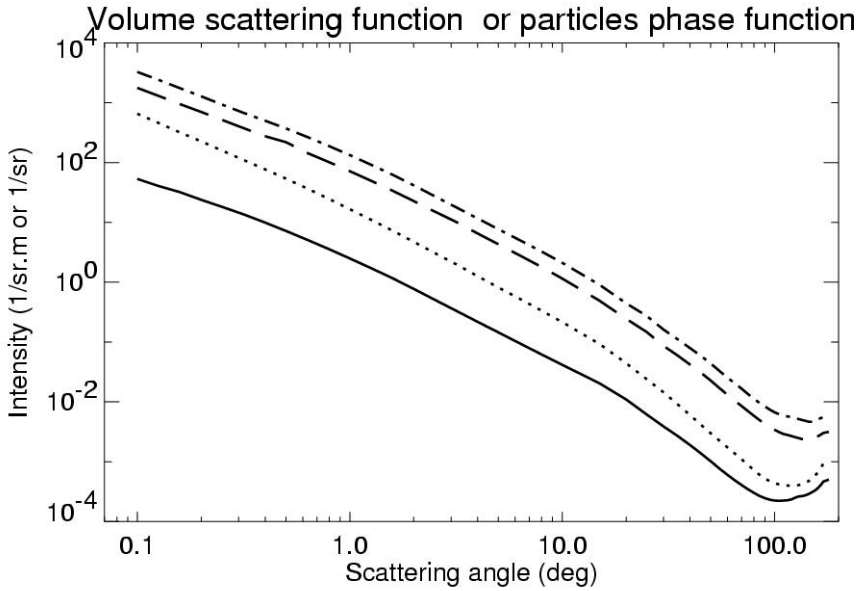

Figure 2.6. volume scattering function from three natural waters measured by *Petzold* (1972) and particles phase function derived by *Mobley et al*. (1993), all at λ=514. The solid line represents clear water, the dotted line represents coastal water, the dash dot line represents turbid water, and the long dashes line represents particles phase function.

The particles phase function derived by *Mobley et al.* (1993) is characterised by a constant back-scattering probability of 1.8 %. It has been recognised that it is not realistic either in Case I waters or in Case II waters. The phase functions of particles in marine environment should have large variability. The shape of the phase function depends on the refractive index and the size distribution of particles. There is a high diversity of the refractive index and the size distribution, depending on the geological origins of the inorganic particles or on the proportion of organic to inorganic particles, especially in coastal waters. It is recognised that uncertainties of the phase function is one of the largest sources of errors, when deriving retrieval methods from RT simulations.

2.2.4. CDOM (Yellow Substance)

CDOM absorbs very strong in the blue domain, but its absorption decrease rapidly with increasing wavelength. Absorption coefficient of CDOM is reasonably well modelled as (*Bricaud et al*., 1981):

$$a_y(\lambda) = a_y(440)e^{-S_y(\lambda-440)}, \tag{2.26}$$

where S_y is empirically determined. Many researchers have reported that the average value of S_y is around 0.014 nm^{-1}(*Bricaud et al*., 1981, *Kishnio et al*., 1984). For the GOMEX and COLOR cruises, an average value of 0.017 nm^{-1} was obtained (*Carder et al.,* 1991). From the

COASTLOOC data, an average value of 0.0176 nm^{-1} was derived (*Babin*, 2000). Figure 2.7 shows the spectrum of CDOM with S_y=0.0176 nm^{-1} and $a_y(440)$=1.0 m^{-1} based on Eq. (2.26).

CDOM is assumed to be a pure absorber.

2.2.5. Classification of Waters

A classification of ocean waters was introduced by *Morel and Prieur* (1977), refined later by *Gordon and Morel* (1983). It is very useful to deal with the retrieval of ocean colour. By definition, ocean waters are divided into two types: Case I and Case II. Case I water are those waters for which phytoplankton and associated products (detritus, CDOM, bacteria) play a dominant role in the variation of optical properties of waters. Case II waters are those waters whose optical properties are influenced not only by phytoplankton and associated products, but also by other substance, such as exogenous particles and exogenous CDOM.

Based on the above definition, Case I water consists of the following optically significant constituents: Phytoplankton and associated particles (endogenous particles), and associated CDOM (endogenous CDOM). Beside the constituents included in Case I waters, Case II waters also consist of exogenous particles, discharged by rivers, or re-suspended from shallow bottom, and the exogenous CDOM from land drainage.

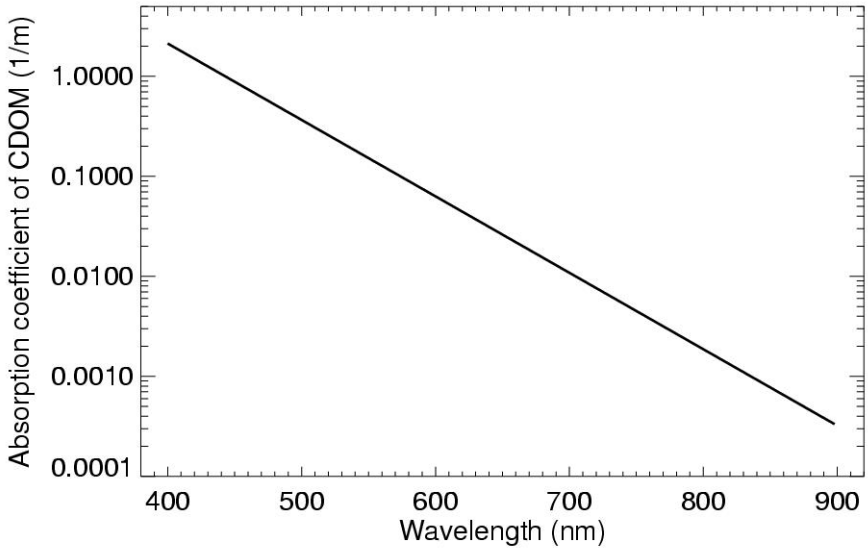

Figure 2.7. Absorption coefficient of CDOM, for $a_y(440)$=1.0m^{-1} and s_y=0.017nm^{-1}

2.3. Radiative Transfer Simulations

Assuming a plane-parallel medium in the ocean-atmosphere system, with a constant input of monochromatic unpolarized radiation at top of atmosphere, the radiative transfer equation may be written as [*Smith,* 1974]:

$$\frac{dL(z,\theta,\phi)}{dr} = -c(z)L(z,\theta,\phi) + L^{*}(z,\theta,\phi) + L^{S}(z,\theta,\phi) \tag{2.27}$$

The term on the left is the rate of change of radiance with distance, r, along the path specified by zenith and azimuthal angles θ and ϕ, at depth z. The net rate of change is the resultant of three processes: loss by attenuation along the direction of travel (c(z) being the value of the beam attenuation coefficient at depth z), gain by elastic scattering of the light initially travelling in other direction(θ′, ϕ′) into the direction (θ, ϕ), and gain by inelastic scattering into the direction (θ, ϕ). The elastic scattering term is given by

$$L^{*}(z,\theta,\phi) = \int_{2\pi} \beta(z,\theta,\phi;\theta',\phi')L(z,\theta',\phi')d\omega(\theta',\phi'), \tag{2.28}$$

where β(z, θ, ϕ) is the volume scattering function of the medium at depth z, and ω is the solid angle.

Because of the mathematical complexity of Eq. (2.27), it must be solved numerically for any realistic situations. MOMO is one of the methods for the above purpose [*Fischer and Grassl*, 1984; *Fell and Fischer*, 2001]. All radiative transfer simulations in this study are performed with the radiative transfer model MOMO. The input needed for MOMO are the IOPs of the atmospheric and oceanic constituents, namely beam attenuation coefficient, single scattering albedo and phase function. This code is based on the Matrix-Operator Method and allows the simulation of the ambient light field in the coupled atmosphere-ocean system. The code is described in detail elsewhere [*Fell and Fischer*, 2001] and just a short introduction into its characteristics will be presented here. The main advantage of the Matrix-Operator method is its efficiency with regard to the simulation of light propagation in optically thick media [*Plass et al*., 1973] and is therefore particularly suited for the development of remote sensing methods regarding the retrieval of water constituents. The code calculates the azimuthally resolved radiance at a discrete number of solar incident and observation zenith angle. The required vertical profiles of the atmospheric and water constituents are introduced through an appropriate number of homogeneous plane parallel layers. Absorption by atmospheric gases is modelled using the modified *k*-distribution approach from *Bennartz and Fischer* [2000]. Reflection at the rough sea surface is modelled according to the statistical description of the wave facet distribution derived by *Cox and Munk* [1954], transmission through the rough sea surface is treated using an approximation introduced by *Fell and Fischer* [2001]. Alternatively, the sea surface may be assumed as flat. Two inelastic scattering processes have been incorporated into the MOMO code: sun-stimulated chlorophyll fluorescence [after *Gordon*, 1976] and Raman scattering [based on *Mobley*, 1994]. Polarisation, CDOM fluorescence and wind direction dependent effects are not taken into account.

The MOMO code has been thoroughly tested and validated through a number of measures [*Fell*, 1997; *Montagner,* 1999, *Fell and Fischer*, 2001]: it has been compared to analytical solutions of the radiative transfer equation for specific simple problems, it has been successfully applied to the canonical problems of oceanic radiative transfer defined in *Mobley et al.* [1993] and has been compared to other codes dealing with the radiative transfer in the atmosphere-ocean system on occasion of a model comparison exercise executed in the frame of the MERIS algorithm development activities. The observed deviations between the MOMO output and the analytical solutions are mostly below 0.1 %, the differences between the compared codes range between <0.1% up to about 5%, depending on the difficulty of the treated problem. These results confirm the suitability of MOMO for the execution of the presented study.

2.4. Artificial Neural Network

A neural network derives its computing power through its massively parallel distributed structure and its ability to learn and therefore to generalise. A neural network is composed of a number of neurons, which are arranged in different network layers and are connected by links. Each link has a numeric weight associated with it. Weights are the primary means of long-term storage in neural networks, and learning usually takes place by updating the weights (*Rumelhart and McClelland*, 1986).

In this thesis, a particular class of ANNs is used, the so-called Multi-Layer Perceptrons (MLPs), to derive the oceanic constituents from ocean colour at the sea level or at top of atmosphere. The MLP used within this study consists of three layers: input layer, one hidden layer and output layer. It has been proved that a neural network with one hidden layer can approximate any continuous function to any arbitrary accuracy given sufficient hidden nodes [*Cybenko*, 1989; *Masters*, 1993]. A bias parameter is added to both input and hidden layer (Figure 2.8). The neurons in the hidden layer are connected with every neuron in the input and output layers. The transfer of information through the MLP can be described by the following equation:

$$\vec{O} = s_c(\mathbf{W^{HO}} \times s_c(\mathbf{W^{IH}} \times \vec{I})), \tag{2.29}$$

where $\vec{I}$ is the input to the MLP, consisting of appropriately pre-processed reflectance values as well as other auxiliary parameters. The weight matrix $\mathbf{W^{IH}}$ contains the weights of all connections between input and hidden layer whereas the weight matrix $\mathbf{W^{HO}}$ contains the weights of all connections between hidden and output layer. At each neuron of hidden and output layer, transition of information is done through the non-linear sigmoidal function, defined by:

$$s_c(x) = \frac{1}{1+\exp(-c_t x)}, \tag{2.30}$$

where c_t is called the temperature constant. The output of the sigmoid defined in Equation (2.30) is confined to the interval [0, 1]. Training of the ANN is done through the back-propagation method, which is a supervised learning technique that compares the responses of the output neurons with the known true responses (training data), traces the errors back through the ANN and readjusts the randomly initialised elements of the weight matrices in order to minimise the multidimensional error function:

$$E = f(\mathbf{W}^{\mathbf{IH}}, \mathbf{W}^{\mathbf{HO}}) . \tag{2.31}$$

In order to test if a trained ANN is able to generalise the functional relationship describing the investigated physical system and has not just found a specific approximation of the offered training data (so called "overfitting", which is comparable to fitting few data with a high-order polynomial), it is applied to another data set (test data) independent of the training data. Only if the absolute error of the ANN output for the test data is within the desired range, the training is deemed successful.

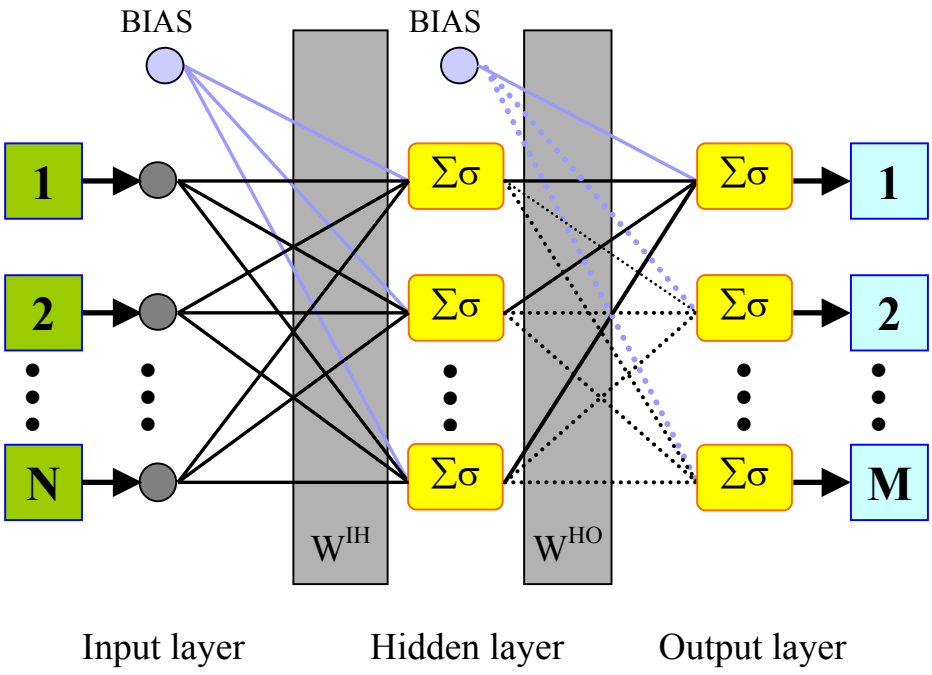

Figure 2.8. Architecture of the Multi-Layer-Perceptron used in this thesis.